

Published in final edited form as:

J Mol Biol. 2008 October 3; 382(2): 385–401. doi:10.1016/j.jmb.2008.07.013.

Engineering a Single Chain Fv Antibody to $\alpha v \beta 6$ Integrin using the Specificity-Determining Loop of a Foot-and-Mouth Disease Virus

Heide Kogelberg^{1,*}, Berend Tolner¹, Gareth J. Thomas², Danielle Di Cara², Shane Minogue³, Bala Ramesh⁴, Serena Sodha¹, Dan Marsh¹, Mark W. Lowdell⁵, Tim Meyer¹, Richard H.J. Begent¹, Ian Hart², John F Marshall², and Kerry Chester¹

¹Cancer Research UK Targeting and Imaging Group, Department of Oncology, Royal Free & University College Medical School, Hampstead Campus, London, NW3 2PF, UK

²Tumour Biology Centre, Cancer Research UK Clinical Centre, Barts and the London Medical and Dental School, Queen Mary's College, John Vane Science Centre Charterhouse Square, London EC1M 6BQ, UK

³Centre for Molecular Cell Biology, Department of Medicine, Royal Free & University College Medical School, Hampstead Campus, London NW3 2PF, UK

⁴Department of Surgery, Royal Free & University College Medical School, Hampstead Campus, London, NW3 2PF, UK

⁵Department of Haematology, Royal Free & University College Medical School, Hampstead Campus, London, NW3 2PF, UK

Summary

The $\alpha v \beta 6$ integrin is a promising target for cancer therapy. Its expression is up-regulated *de novo* on many types of carcinoma where it may activate transforming growth factor- $\beta 1$ and transforming growth factor- $\beta 3$, interact with the specific extracellular matrix proteins and promote migration and invasion of tumour cells. The viral protein 1 (VP1) coat protein of the O₁ British field strain serotype of foot-and-mouth disease virus is a high-affinity ligand for $\alpha v \beta 6$, and we recently reported that a peptide derived from VP1 exhibited $\alpha v \beta 6$ -specific binding *in vitro* and *in vivo*. We hypothesized that this peptide could confer binding specificity of an antibody to $\alpha v \beta 6$. A 17-mer peptide of VP1 was inserted into the complementary-determining region H3 loop of MFE-23, a murine single-chain Fv (scFv) antibody reactive with carcinoembryonic antigen (CEA). The resultant scFv (B6-1) bound to $\alpha v \beta 6$ but retained residual reactivity with CEA. This was eliminated by point mutation (Y100bP) in the variable heavy-chain domain to create an scFv (B6-2) that was as structurally stable as MFE-23 and reacted specifically with $\alpha v \beta 6$ but not $\alpha 5 \beta 1$, $\alpha v \beta 3$, $\alpha v \beta 5$, $\alpha v \beta 8$ or CEA. B6-2 was internalized into $\alpha v \beta 6$ -expressing cells and inhibited $\alpha v \beta 6$ -dependent migration of carcinoma cells. B6-2 was subsequently humanized. The humanized form (B6-3) was obtained as a non-covalent dimer from secretion in *Pichia pastoris* (115 mg/l) and was a potent inhibitor of $\alpha v \beta 6$ -mediated cell adhesion. Thus, we have used a rational stepwise approach to create a humanized scFv with therapeutic potential to block $\alpha v \beta 6$ -mediated cancer cell invasion or to deliver and internalize toxins specifically to $\alpha v \beta 6$ -expressing tumours.

*Corresponding author. h.kogelberg@ucl.ac.uk.

[†]Present address: H. Kogelberg/B. Tolner/D. Marsh/R.H.J. Begent/ K. Chester, UCL Cancer Institute, The Paul O'Gorman Building, University College London, 72 Huntley Street, London, WC1E 6BT, UK

Keywords

antibody engineering; scFv; integrin $\alpha v\beta 6$; VP1 peptide; foot-and-mouth disease virus

Introduction

Integrins are a family of heterodimeric class I transmembrane receptors that comprise an α subunit and β subunit in non-covalent association.¹ They mediate cell-matrix and cell-cell interactions involving adhesion, proliferation, migration and invasion. These processes underpin many normal and pathological events, including embryonic development, wound healing, inflammation and tumour growth as well as metastasis.¹⁻⁴

$\alpha v\beta 6$ is an epithelial cell-restricted integrin that shows *de novo* expression in many carcinomas.^{2,5-8} Known biological roles of $\alpha v\beta 6$ include binding to extracellular matrix proteins (fibronectin, vitronectin and tenascin), which facilitates migration of $\alpha v\beta 6$ -expressing cells,⁵ and generation of active transforming growth factor (TGF)- $\beta 1$ and TGF- $\beta 3$, which is mediated by $\alpha v\beta 6$ binding to the latency associated protein (LAP) of the TGF- β complex.⁹ There is growing evidence⁵ that $\alpha v\beta 6$ expression is functionally linked to malignant progression: elevated expression of $\alpha v\beta 6$ is associated with significantly reduced survival time of patients with colorectal carcinoma,¹⁰ those with cervical carcinoma¹¹ and those with non-small cell lung cancer;¹² transcriptional activation of $\beta 6$ and subsequent expression of $\alpha v\beta 6$ have been observed during the epithelial-mesenchymal transition, which is thought to allow cells to acquire a more aggressive phenotype,¹⁰ and, in oral squamous cell carcinomas, expression of $\alpha v\beta 6$ in a poorly invasive cell line leads to increased migration on fibronectin and invasion through a reconstituted basement membrane.¹³ These accumulated data strongly indicate a pro-invasive role for $\alpha v\beta 6$ and, combined with the evidence of selective tumour expression,^{2,5-8} make $\alpha v\beta 6$ a very promising new target for cancer treatment.

Antibodies have had notable success in targeting tumour cell surface antigens.¹⁴ Current clinical use is mainly restricted to monoclonal antibodies (murine or humanized), but recombinant antibody-based treatments are becoming increasingly available and offer exciting new possibilities.^{15,16} We aimed to engineer a recombinant antibody with potential to inhibit the biological activity of $\alpha v\beta 6$ and to deliver a toxic payload specifically to $\alpha v\beta 6$ -expressing cancer cells. The single-chain Fv (scFv) antibody fragment format was selected because scFvs are the smallest fragment to retain the full binding structure of a native antibody, and they are readily engineered to express as fusion proteins with natural effectors or toxic agents.^{15,16} scFv consist of the variable heavy-chain (VH) and variable light-chain (VL) regions of an antibody tethered by a flexible linker. Each scFv contains six complementarity-determining regions (CDRs) of varying lengths and sequence; these determine antigen recognition and are stabilized by relatively conserved framework regions. We reasoned that an $\alpha v\beta 6$ ligand could function as a CDR if suitably engineered into supporting scFv frameworks.

The viral protein 1 (VP1) of the foot-and-mouth disease virus (FMDV) serotype O₁ British field strain¹⁷ is a known ligand for $\alpha v\beta 6$. In cattle, the integrin is expressed constitutively on certain normal epithelial cells where it is thought to act as receptor for attachment and uptake of the virus.¹⁸⁻²⁰ Tropism of the FMDV for $\alpha v\beta 6$ is mediated in part by the arginine-glycine-aspartic acid (RGD) sequence followed by two leucines (L) to give an RGD β XXL motif.²¹ Potency and specificity of VP1 for $\alpha v\beta 6$ are remarkably high and surpass that of the LAP.²¹⁻²³

FMDV peptides have been shown for many years to inhibit integrin functions; more recently, 17-mer and 20-mer peptides of VP1 containing an RGD_{LXXL} motif were identified as potent inhibitors of FMDV binding to purified $\alpha v\beta 6$ and to $\alpha v\beta 6$ -expressing cells (Ref. 21 and references therein) and a 20-mer VP1 peptide (A20FMDV2) with this motif that inhibited binding of $\alpha v\beta 6$ to LAP.²⁴ We proposed that this evolutionary-optimized VP1 sequence could be exploited to define binding specificity of an antibody to $\alpha v\beta 6$. MFE-23, an existing scFv, was selected as a scaffold to test this hypothesis. MFE-23 is a favourable starting point as it is structurally well defined,²⁵ including its interaction with cognate antigen, carcinoembryonic antigen (CEA), and it has a proven high performance in a number of clinical trials.²⁶⁻³⁰ The third variable loop of the heavy chain (CDR-H3) of MFE-23 provides the major site of interaction with CEA, as assessed by mutagenesis,³¹ and was therefore the preferred site for insertion.

We describe a series of anti- $\alpha v\beta 6$ scFvs generated by insertion of a 17-mer peptide of VP1, comprising the inhibiting 20-mer peptide²⁴ minus the first N-terminal and two C-terminal residues, into CDR-H3. First the murine MFE-23 was used as a scaffold because this enabled direct structural and functional comparisons of the new anti- $\alpha v\beta 6$ scFvs with an existing well characterized molecule. We then showed that the murine scaffold was exchangeable with a humanized framework and that $\alpha v\beta 6$ binding was maintained. The humanized anti- $\alpha v\beta 6$ scFv has potential as a therapeutic to inhibit $\alpha v\beta 6$ -mediated functions or to specifically target $\alpha v\beta 6$ -expressing tumours.

RESULTS

Changing the target specificity of MFE-23 from anti-CEA to anti- $\alpha v\beta 6$

DNA encoding the 17-mer peptide sequence from A₁₄₀ to A₁₅₆ of VP1 was inserted at the tip of CDR-H3 of MFE-23, between T₉₈ and G₉₉ (Kabat nomenclature) as depicted in Fig. 1, to generate the gene for B6-1, the first of a series of anti- $\alpha v\beta 6$ scFvs. B6-1 protein was expressed and purified from *Escherichia coli* and when tested by ELISA showed concentration-dependent binding to $\alpha v\beta 6$ (Fig. 2a). In agreement with cation-dependent integrin-ligand binding, B6-1 did not bind in the presence of ethylenediaminetetraacetic acid (EDTA) (Fig. 2b). Binding of the B6-1 scFv to $\alpha v\beta 6$ on the surface of cells was investigated by flow cytometry using $\alpha v\beta 6$ positive A375P $\beta 6$ cells in comparison with A375Ppuro $\alpha v\beta 6$ -negative cells. The results demonstrated specific concentration-dependent binding of B6-1 to the $\beta 6$ -transfected cells as illustrated in Fig. 2c (bottom left panel). Observed fluorescence shifts were similar for B6-1 at 5- and 0.5 $\mu\text{g/ml}$ concentrations, indicating that B6-1 reached almost-saturation levels of binding at 0.5 $\mu\text{g/ml}$. Tropism for $\alpha v\beta 6$ was shown to be mediated by the inserted VP1 peptide because the parent scFv, MFE-23, did not bind to either of these cell lines (Fig. 2c, top left and top right panels).

Lack of binding of B6-1 to A375Ppuro cells indicates specificity for $\alpha v\beta 6$, because although A375Ppuro cells do not express $\alpha v\beta 6$, they do express other RGD-directed integrins, namely, $\alpha v\beta 8$, $\alpha v\beta 5$, $\alpha v\beta 3$ and $\alpha 5\beta 1$, at levels similar to those with the $\beta 6$ -expressing A375P $\beta 6$ cells (Fig. 3a). The lack of detectable binding of B6-1 to A375Ppuro cells indicates that, as far as is detectable by flow cytometry, B6-1 did not cross-react with the other four integrins. These findings were consistent with experiments showing that B6-1 did not bind to immobilized $\alpha v\beta 3$ on ELISA plates, although a strong signal was obtained with $\alpha v\beta 6$ (Fig. 3b). The parent scFv, MFE-23, did not bind to either $\alpha v\beta 3$ or $\alpha v\beta 6$. Immobilization of both integrins to the wells was confirmed with an anti- αv antibody (Fig. 3b). In further support of the specificity of B6-1 binding to $\alpha v\beta 6$, we investigated whether this binding could be inhibited by the function-blocking anti- $\alpha v\beta 6$ antibody 10D5 or the 20-mer VP1 peptide²⁴ that contains amino acids identical with the 17-mer inserted into the VH CDR3 loop of MFE-23 to give B6-1. Figure 3c shows that the function-blocking anti- $\alpha v\beta 6$

antibody and the 20-mer VP1 peptide inhibited binding of B6-1 to immobilized $\alpha v \beta 6$. The function-blocking anti- $\alpha v \beta 3$ antibody, however, was not an inhibitor in this assay. Binding of B6-1 to $\alpha v \beta 6$ was also inhibited by the function-blocking anti- $\alpha v \beta 6$ antibody when $\alpha v \beta 6$ was expressed on the surface of cells that also expressed integrins $\alpha v \beta 8$, $\alpha v \beta 5$, $\alpha v \beta 3$ and $\alpha 5 \beta 1$ (Fig. 3d). However, in the same experiments, the function-blocking anti- $\alpha v \beta 3$ antibody had no inhibitory effect on this binding. These data provide further support of the specificity of B6-1 for $\alpha v \beta 6$.

Next, we investigated whether B6-1 could functionally inhibit $\alpha v \beta 6$ -dependent migration of cells to LAP. We used VB6 cells as their migration towards LAP is solely mediated through $\alpha v \beta 6$.³² The function-blocking $\alpha v \beta 6$ specific antibody 10D5 was used as a positive control (Fig. 4a and b). Inhibition potential of the scFv B6-1, was compared with the 20-mer VP1 peptide A20FMDV2.²⁴ Addition of 50 $\mu\text{g/ml}$ (1.75 μM) of B6-1 to VB6 cells was shown to considerably inhibit migration towards LAP when compared to MFE-23 (Fig. 4a). Inhibition was concentration dependent (Fig. 4b) and apparent at 100 nM, whereas the peptide showed no inhibition when used at 10-fold higher concentrations, i.e. at 1 μM (Fig. 4c). The peptide inhibited migration of VB6 cells when used at 10 or 100 μM (Fig. 4c). In this assay, therefore, the scFv B6-1 was more potent than the 20-mer VP1 peptide. Taken together, the experiments with B6-1 confirmed our hypothesis that a peptide sequence from VP1 could be used to create a biologically active anti- $\alpha v \beta 6$ scFv.

Elimination of residual binding to CEA

The reactivity of the B6-1 parental scFv (MFE-23) was directed against CEA; therefore, binding of B6-1 to CEA was investigated. ELISA experiments showed residual concentration-dependent reactivity of B6-1 with CEA (Fig. 3a, middle panel), although considerably below that obtained with MFE-23 (Fig. 5a, left panel). This was addressed by introduction of a Y100bP mutation in CDR-H3, yielding a second scFv, B6-2, which was expressed in *E. coli* and in the yeast *Pichia pastoris*. The size-exclusion chromatographic profiles of the expressed proteins from both organisms were superimposable (Fig. 5b) and showed that B6-2 eluted as two distinct peaks, representing the monomeric form and a non-covalently associated dimeric form of the scFv. The monomeric form was used for all subsequent experiments and when tested by ELISA showed no binding to CEA (Fig. 5a, right panel). Consistent with ELISA, B6-2 also showed no binding to the CEA-expressing LS174T cells as the observed fluorescence intensity was equal to that of the omission control (Fig. 5c). These results indicate that the Y100bP mutation in B6-2 had successfully eliminated all residual binding of the scFv to CEA. In addition, the Y100bP mutation did not cause cross-reactivity with $\alpha v \beta 3$, as shown by ELISA (Fig. 3b), or with $\alpha v \beta 8$, $\alpha v \beta 5$, $\alpha v \beta 3$ and $\alpha 5 \beta 1$, as shown by lack of binding to A375Ppuro cells (which express these integrins; see ‘*Changing the target specificity of MFE-23 from anti-CEA to anti- $\alpha v \beta 6$* ’) by flow cytometry (Fig. 5d). This mutation had also no detrimental effects on biological activity, because B6-2 bound as least as well as B6-1 to immobilized $\alpha v \beta 6$ in ELISA (Fig. 3b) and was able to inhibit $\alpha v \beta 6$ -mediated cell migration towards LAP in the Transwell assay in a similar manner as B6-1 (Fig. 4a and c).

Interestingly, although B6-1 binding to immobilized CEA on ELISA was substantially below that of MFE-23, this was not the case when the scFvs were tested by flow cytometry on CEA-expressing cells. Here, experiments showed that B6-1 bound to the human colon adenocarcinoma cell line LS174T with a shift in fluorescence intensity only slightly below that of MFE-23. The gated cells that are present in the fluorescence intensity window of $7 \times 10^1 - 10^4$, as indicated in Fig. 5c, were 31.6% for MFE-23 and 26.0% for B6-1.

Structure and stability of B6-2

We investigated whether insertion of the 17-mer VP1 peptide and subsequent Y100bP mutation had affected the structure and stability of the protein in comparison with MFE-23. The B6-2 second derivative Fourier transform infrared (FT-IR) spectrum showed a strong band at 1635 cm^{-1} , in agreement with a protein which consists mainly of β -sheet and as shown previously in the X-ray structure of MFE-23.²⁵ Indeed, the spectra of B6-2 and MFE-23 were superimposable as shown in Fig. 6a, indicating that insertion of the VP1 peptide was not detrimental to protein structure. The intensity of the β -sheet band at 1635 cm^{-1} was used to monitor stability of the protein, because with increasing temperature, this band will reduce in intensity as an indicator of the protein denaturation. Recording of the denaturing curve and fitting to a sigmoidal curve gave a midpoint of denaturation of $45\text{ }^{\circ}\text{C}$ for B6-2 (Fig. 6b). For MFE-23, this temperature was $47\text{ }^{\circ}\text{C}$, as was previously reported.³³ The FT-IR results confirmed that B6-2 had very similar stability to the parent scFv.

Internalization of B6-2 into $\beta 6$ -transfected A375P cells

For drug development, it is important to know whether the scFv has potential to internalize specifically into cells expressing $\alpha v\beta 6$. Therefore, we next investigated whether binding of B6-2 to $\alpha v\beta 6$ on the cell surface resulted in internalization of the scFv. A375P $\beta 6$ cells were incubated with B6-2 at $4\text{ }^{\circ}\text{C}$ to allow adsorption but prevent endocytosis. After they were washed, cells were incubated at $37\text{ }^{\circ}\text{C}$ to follow the internalization of surface-bound scFv. Results demonstrated that after 10 min of incubation at $37\text{ }^{\circ}\text{C}$, the B6-2 scFv (red in Fig. 7) was predominantly localized to the plasma membrane (Fig. 7b-d). However, after 3 h of incubation, in addition to some plasma membrane staining, B6-2 localized to numerous intracellular puncta (Fig. 7f-h). B6-2 was also found to localize to similar puncta at 30-min and 1-h time points (data not shown). Control images acquired using identical conditions with the $\alpha v\beta 6$ -negative A375Ppuro cells showed little or no internalisation at 10 min (Fig. 7j-l) or 3 h (Fig. 7n-p). There was also no significant signal with the $\alpha v\beta 6$ -positive cells when B6-2 was omitted from the experiment (data not shown). These results indicated that binding of B6-2 was specific for $\alpha v\beta 6$ on the cell surface and that binding to $\alpha v\beta 6$ was followed by internalization.

Humanization

Although we had successfully demonstrated that B6-2 had the required properties of its rational design, the MFE-23 scaffold used to create B6-2 is murine in origin and is predicated to lead to production of human anti-mouse antibodies if used repeatedly in patients. We therefore set out to create a humanized version of B6-2 using the previously described stabilized humanized MFE-23 (shMFE)³⁴ as a scaffold.

B6-3, the humanized variant and third of the series of anti- $\alpha v\beta 6$ scFvs, was expressed by *P. pastoris* with a yield of 115 mg/l after initial expanded-bed immobilized metal-affinity chromatography (IMAC). Interestingly, unlike B6-2, which was largely obtained in monomeric form (Fig. 5b), the B6-3 protein formed predominantly a non-covalent dimer when analyzed by size-exclusion chromatography (data not shown). The purified dimer retained a single peak after freeze thawing (Fig. 8a) and was remarkably stable in dimeric form in that it was not separated into monomer by either 3 M urea, or acidic and basic pH.

B6-3 bound to immobilized $\alpha v\beta 6$ in ELISA in a similar fashion to B6-2 (Fig. 8b). Furthermore, B6-3 inhibited the $\alpha v\beta 6$ -dependent adhesion of [^{51}Cr] $\alpha v\beta 6$ -expressing 3T3 $\beta 6.19$ fibroblasts to LAP in a concentration-dependent manner (Fig. 8c). The potency of the dimeric B6-3 as an inhibitor ($\text{IC}_{50} = 196.2 \pm 27.6\text{ nM}$) was higher than that of the A20FMDV2 VP1 peptide ($\text{IC}_{50} = 589.6 \pm 101.0\text{ nM}$) and that of the monomeric scFv, B6-2 ($\text{IC}_{50} = 483.5 \pm 40.5\text{ nM}$). MFE-23 was used as a negative control in these experiments and

showed no inhibition of adhesion. The 10D5 murine $\alpha v \beta 6$ function-blocking antibody was used as a positive control (Fig. 8c).

DISCUSSION

The $\alpha v \beta 6$ integrin is an emerging cancer target that is expressed on epithelial cells and associated with extracellular matrix interactions. We aimed to engineer a recombinant scFv antibody with specificity for $\alpha v \beta 6$, and we used an evolutionarily optimized RGDLXXL-containing 17-mer sequence from FMDV to achieve this goal. We first showed that the peptide could alter the tropism of MFE-23, an anti-CEA scFv, when inserted into CDR-H3. It was predicted that the peptide would confer specificity to $\alpha v \beta 6$ because, in $\beta 6$ -transfected cells, $\alpha v \beta 6$ functions as the major receptor for virus attachment, whereas other epithelial expressed integrins, namely, $\alpha 5 \beta 1$ and $\alpha v \beta 5$, appear not to have a role.³⁵ Our results confirmed the predictions because, when the 17-mer was inserted into MFE-23, the resulting scFv loop variant (B6-1) was specific for $\alpha v \beta 6$ and inhibited its biological activity.

The next stage was to detect and eliminate any residual binding of the scFv to CEA. This was readily achieved by the Y100bP mutation in the VH domain to create a non-CEA binding variant, B6-2. The mutation was based on previous work that showed that binding of MFE-23 to CEA was abolished by this mutation.³¹ The interaction of MFE-23 with CEA was predicted from the MFE-23 crystal structure and from modelling.^{25,36} Reassuringly, in our current experiments, FT-IR analysis indicated that insertion of VP1 and Y100bP mutation was not detrimental to the overall structure of the scFv. Stability is of major importance for therapeutics, and FT-IR showed that B6-2 was of similar stability to parent scFv, MFE-23, which has been used successfully in the clinic.

Having established proof of concept by comparison of our anti- $\alpha v \beta 6$ scFvs with the well-characterized MFE-23, we set out to address the issue of potential immunogenicity. B6-2 is of murine origin, and our ultimate aim was to create an scFv with potential to deliver cancer therapy; therefore, the last stage was to create a humanized version of B6-2. A rational basis for humanizing mutations had been provided by comparison of the X-ray structure of MFE-23 with a human analogue that suggested 28 surface residues suitable for humanization.²⁵ These residues, when introduced into MFE-23, combined with three additional mutations produced shMFE.³⁴ In our current study, shMFE was shown to be a suitable scaffold for insertion of the VP1 peptide. B6-3, the resulting humanized scFv, was naturally almost entirely dimeric and appeared to be a better inhibitor of $\alpha v \beta 6$ -dependent cell binding to LAP than the VP1 peptide, A20FMDV2, or the monomeric scFv, B6-2. scFvs are readily amenable to genetic manipulation, resulting in variants with higher affinity or specificity for target, for example, as we have shown with shMFE using yeast display.³⁴ Therefore, as it is beyond the scope of this current study, future work could include creation of optimized humanized anti- $\alpha v \beta 6$ antibodies, fully characterized in terms of integrin cross-reactivity. This could be achieved by using libraries of scFvs with CDRs grafted with different peptides, loop lengths or flanking regions³⁷ and by utilizing further CDR loops. The system also has potential for peptide insertion into other protein scaffolds.

The loop grafting approach to making a new humanized scFv that we have taken is unusual. Antibodies with specificity for their target have been classically obtained by hybridoma screening technology after immunization with the antigen³⁸ or, in the case of scFvs, by phage technology where repertoires of scFvs are displayed on the surface of filamentous bacteriophage and screened for binding to antigen.³⁹ There are a small number of antibodies reported to have been successfully generated using a structure-based approach, although usually by replacement of CDR loops rather than addition of amino acids to these loops. For example, a DNA-binding antibody has been generated by replacing CDR-H3 with a

sequence from a class B basic helix-loop-helix protein.⁴⁰ In a further study, peptides of the cellular prion protein, believed to be involved in binding to the abnormal scrapie prion protein conformation, were grafted into CDR-H3 of an immunoglobulin G (IgG) antibody that is specific for the envelope glycoprotein of HIV-1.⁴¹ The resultant antibodies bound specifically to disease-associated conformations of prion protein and not to the HIV-1 envelope. In some cases, the functional activity of peptide-grafted antibodies has been improved by simultaneous grafting more than one peptide into various CDR loops. An anti-tumor necrosis factor (TNF)- α domain antibody, for example, was obtained by displaying simultaneously three peptides on the VH region of a human antibody.⁴² The antibody bound to TNF- α and inhibited the interaction of TNF- α with its two receptors, TNFR1 and TNFR2, reduced the TNF- α -mediated cytotoxicity and inhibited TNF- α -mediated caspase activity. In another instance, a peptide with cMpl receptor-binding capability was first grafted individually into different CDRs of a fully human scaffold.³⁷ Optimal presentation within the scaffold was selected by randomising two amino acids flanking each end of the grafted peptide and phage display and biopanning. A Fab fragment with two peptides showed agonistic activity in an *in vitro* cMpl receptor signaling assay and was able to effectively stimulate platelet production in mice.

In our study we added a 17-mer peptide of VP1 to the existing CDR-H3 of MFE-23. We reasoned that this would give maximal accessibility for binding to $\alpha v\beta 6$, based on the X-ray structure of FMDV, which revealed that the $\alpha v\beta 6$ -recognizing RGD₂ motif is located on a long highly mobile loop between β -strands G and H and forms a self-contained unit.¹⁷ Similarly, in fibronectin, a further ligand for $\alpha v\beta 6$, the RGD loop is highly mobile, protruding from the rest of the 10th type III module.⁴³ The insertion of a target-binding peptide sequence into an existing loop is a rather rarely used approach. Two previous examples are the insertion of three RGD repeats into the CDR3 of an immunoglobulin human/mouse chimeric heavy chain to create a chimeric antibody that recognized specifically the integrin $\alpha v\beta 3$ and the insertion of a peptide from the CD4 receptor to give an antibody that was subsequently used as an immunogen to generate murine monoclonal antibodies to the receptor.⁴⁵ However, to our knowledge, the CDR insertion method has not been previously used to create function-blocking recombinant scFvs.

B6-3, the rationally designed humanized scFv created with our approach, has potential to form the basis for new anti-cancer therapies because its target, the $\alpha v\beta 6$ integrin, is linked with carcinoma progression due to its ability to modulate invasion, inhibit apoptosis, regulate protease expression and activate TGF- $\beta 1$ and TGF- $\beta 3$. B6-3 could be used to specifically deliver toxic agents since $\alpha v\beta 6$ is *de novo* expressed on various cancerous tissues, and the scFvs we created were specifically internalized into $\alpha v\beta 6$ -expressing cells.

We have also shown that the MFE-23 scFv can be modified to provide a stable non-CEA-binding humanized scaffold. This has potential to provide a platform technology for creating scFvs to a range of targets, in particular, when the specificity-determining region of the ligand is known and can be exploited as a CDR. In theory, other CDRs may be employed and higher specificity/affinity obtained by mutation and selection using standard antibody engineering technology.⁴⁶

Materials and Methods

Antibodies

Murine monoclonal antibodies to $\alpha v\beta 3$ (LM609), $\alpha v\beta 6$ (10D5), $\alpha 5\beta 1$ (P1D6) and αv (P3G8) were purchased from Chemicon International. Antibodies to $\alpha v\beta 5$ (P1F6) and $\alpha v\beta 8$ (14E5) were generous gifts from Drs. Dean Sheppard and Steve Nishimura (University of California, San Francisco, San Francisco, CA), respectively. Antibody W6/32 (anti-major

histocompatibility complex class 1) was a generous gift from Sir W. Bodmer (Institute of Molecular Medicine, Oxford). MFE-2325,26 and shMFE34 were described previously; polyclonal rabbit anti-MFE IgG antibody was produced in the University College London Department of Oncology.

Three-dimensional protein visualisation

The X-ray structure of MFE-23 (Protein Data Bank code 1QOK)²⁵ was visualized in Insight II (Accelrys) on a Silicon Graphics workstation.

Primer synthesis and sequence analysis

All primers were ordered from and sequencing reactions were performed by MWG (Biotech AG).

Cell lines

A375P β 6 is an α v β 6-positive cell line obtained by retroviral transduction of melanoma cells with human β 6 cDNA and the puromycin-resistance gene as described previously.²⁴ Control A375Ppuro cells were transduced with the puromycin-resistance gene alone.²⁴ VB6 is a well-characterized α v β 6-expressing oral squamous cell carcinoma cell line.⁴⁷

Nomenclature

B6-1 is MFE-23 with a 17-mer peptide of VP1 inserted into CDR-H3 to confer α v β 6 reactivity. B6-2 is B6-1 with additional Y100bP in the VH domain. B6-3 is a humanized version of B6-2.

E. coli expression

The gene encoding the B6-1 scFv was constructed by PCR insertion of a 51-bp fragment, encoding a 17-mer peptide harboring the α v β 6-binding sequence of VP1, into CDR-H3 of MFE-23 (Fig. 1). First, the 5' fragment was constructed using primers: VH B6-1 sense 5'-**CATGCCATGGCCCAGGTGAACTG**-3' containing an *Nco*I site (underlined in bold) and VH B6-1 anti-sense 5'-GCGCCAGCACCTGCAGATCACCTCGCAGATTCGGAAGTGCAGTCGGAGTCCCCTCATTAC-3' containing parts of the α v β 6-binding motif. Second, the 3' B6-1 fragment was constructed using primers: VL B6-1 sense 5'-**CTGCGAGGTGATCTGCAGGTGCTGGCCGAGAAAGTTGCAGGGCCGTACTACTTTGACTACTG**-3' containing overlapping regions with VH B6-1 anti-sense primer (shown underlined) and the remaining parts of the α v β 6-binding motif and VL B6-1 anti-sense 5'-**ATAGTTTATAGCGGCCGCCGTTTCAGCTC**-3' containing a *Not*I site (bold and underlined). Finally, the PCR products from the first two reactions were used as templates and amplified with the primers: VH B6-1 sense and VL B6-1 anti-sense to give the full-length B6-1 gene flanked by *Nco*I and *Not*I sites. The final PCR product was cloned *Nco*I/*Not*I (downstream of a *PeB* leader sequence) into the respective sites of a pUC119 derivative with a C-terminal hexahistidine tag (His-tag).⁴⁸ The fragment encoding B6-1 in the resulting plasmid (pB6-1) was verified by DNA sequencing.

The Y100bP mutation in VH B6-1 was introduced by site-directed mutagenesis of pB6-1 using 5'-GTTGCAGGGCCGTACCCGTTTGACTACTGGGGC-3' sense and 5'-GCCCCAGTAGTCAAAC**CGGGTACGGCCCTGCAAC**-3' anti-sense primers (proline encoding nucleotide sequence is shown in bold) to give pB6-2. Success of mutation was confirmed by DNA sequencing.

The pB6-1 and pB6-2 plasmids were electroporated into competent *E. coli* TG1 cells and grown on agar plates containing 2x YT, 50 µg/ml ampicillin and 1% glucose at 37 °C. Single colonies were used to inoculate 5 ml of 2x YT, 50 µg/ml ampicillin and 1% glucose. After overnight incubation, the cultures were used to inoculate (1:500) 2x 500ml of 2x YT, 50 µg/ml ampicillin and 0.05% glucose. The 500-ml cultures were grown at 37 °C until OD₆₀₀ was 0.9, at which point protein expression was induced by addition of 1 mM IPTG (isopropyl-β-D-thiogalactoside), and growth was continued at 30 °C overnight. The supernatant (approximately 1 l) was separated from the cells by centrifugation at 16,000g for 25 min at 4 °C, further clarified by filtration through 0.2 µm membranes (Nalgene), dialyzed into phosphate-buffered saline (PBS) and adjusted to 1 M NaCl. B6-1 and B6-2 scFvs were purified from the dialyzed supernatant by IMAC as follows. 10 ml of Cu²⁺-charged Streamline™ chelating resin (GE Healthcare) was incubated with the above supernatant, under agitation. After 1 h at room temperature, the resin was washed with 1 M NaCl/PBS, pH 7.4, followed by 40 mM imidazole, pH 7.4. Bound proteins were eluted with 200 mM imidazole, pH 7.4, dialyzed against Tris-buffered saline (TBS), pH 7.5, concentrated by an Amicon stirred cell with a YM3 membrane (Millipore) and further purified by Superdex 75 (125-ml bed volume; GE Healthcare) size-exclusion chromatography in TBS, pH 7.5. The column was calibrated with molecular-weight standards, ovalbumin (44,000), carbonic anhydrase (29,000), and myoglobin (17,000).

P. pastoris expression

The plasmid harbouring the B6-3 gene was constructed essentially as described above for B6-1 but with the variation that shMFE34 was used as a starting scFv and the Y100bP mutation was included in the second PCR step. Primers used for the 5' fragment were: VH B6-3 sense 5'-CATGCCATGGCCCAAGTTAACTGGAACAGTCC-3' (*Nco*I site, bold and underlined) and VH B6-3 anti-sense 5'-GAGCCAGCACCTGCAGATCACCTCGCAGATTCGGAACAGTGGTGTCCCTTCGTTGC-3'. Primers used for the 3' fragment were: VL B6-3 sense 5'-CTGCGAGGTGATCTGCAGGTGCTGGCTCAGAAAGTTGCAGGTCCTTACCCTTTCGACTACTGGGGACAAGG-3' (overlap with VH B6-3 anti-sense, underlined; Y100bP mutation, bold and underlined) and VL B6-3 anti-sense 5'-ATAGTTTAGCGGCCGACGCTTGATTTC-3' (*Not*I site, bold and underlined). VH B6-3 sense and VL B6-3 anti-sense were used to generate the full-length B6-3 gene that was cloned *Nco*I/*Not*I into the pUC119 derivative as above. The fragment encoding B6-3 in the resulting plasmid (pB6-3) was verified by DNA sequencing. The pB6-2 and pB6-3 plasmids were digested with *Sfi*I and *Not*I and cloned into equally digested pPICZα.BHis or pPICZα.BCysHis vectors, respectively, for expression in yeast. The vectors are modified from pPICZα.B vector (Invitrogen) in that they do not express the myc-tag; pPICZα.BCysHis also contains a Cys immediately before the six His residues. The plasmids were linearized with *Pme*I and transformed into electrocompetent X33 cells (Invitrogen) by electroporation. Transformants were grown on YPDS and Zeocin (100 µg/ml, Invitrogen) plates. Single colonies were screened by PCR with the 5' AOX and 3' AOX primers (Invitrogen) to confirm insertion of pB6-2 or pB6-3 in the yeast AOX1 gene. Positive clones were selected and screened for methanol-induced protein expression according to the manufacturer's recommendation (Invitrogen). Clones with the highest protein expression were used to produce seed lots for medium-scale protein production by fermentation with initial purification using expanded bed adsorption IMAC essentially as previously described. 49,50 His-tagged scFvs in the 200 mM imidazole IMAC eluate were further concentrated by application to a 1 ml Ni²⁺-charged HiTrap IMAC HP column (GE Healthcare) according to the manufacturer's instructions. The eluted proteins were finally purified by size-exclusion chromatography on a Superdex 75 column (125 ml bed volume) in PBS, pH 7.4.

SDS-PAGE

Proteins were analyzed by SDS-PAGE using Tris/glycine gels (12%, Invitrogen) and stained with Coomassie brilliant blue (R250).

Binding of MFE-23 CDR-H3 variants to immobilized $\alpha\nu\beta 6$ and $\alpha\nu\beta 3$ by ELISA

Ninety-six-well plates (Nunc-Immuno™ Plates, Maxi Sorp, Nalgen Nunc International) were coated with either 3 $\mu\text{g/ml}$ of $\alpha\nu\beta 6$ or $\alpha\nu\beta 3$ (Chemicon International) in TBS, pH 7.5. The $\alpha\nu\beta 6$ was prepared from CHO $\alpha\nu\beta 6$ cells (a kind gift from Dr Dean Sheppard, University of California, San Francisco) to approximately 95% purity as described previously⁵¹ (Supplementary Fig. 1). The $\alpha\nu\beta 3$ was validated by the supplier as functional for ligand binding (vitronectin, von Willebrand Factor, fibrinogen, and fibronectin) in ELISA. Plates were washed two times with 0.1 % Tween-20 (in TBS) followed by eight washes with TBS and blocked with 5% skimmed dried milk in TBS. All subsequent washes were performed in a similar manner but using TBS containing 1 mM MgCl_2 , 1 mM MnCl_2 and 1 mM CaCl_2 (TBSM). Secondary and tertiary antibodies for MFE-23 derived scFvs were rabbit anti-MFE-23 IgG (1:1000 dilution) and horseradish peroxidase (HRP)-conjugated goat anti-rabbit IgG (1:1000 dilution; Sigma), respectively. The secondary antibody for mouse anti- $\alpha\nu$ was sheep HRP-labeled anti-mouse IgG (1:1000 dilution; GE Healthcare). Plates were washed between each incubation. HRP was detected with *o*-phenylenediamine dihydrochloride (Sigma) in citrate buffer, pH 5.0, and the reactions were stopped with 4M HCl. Absorbance was read at 490 nm on a plate reader (OPSYS MR, Dynex Technologies). All incubations were performed for 1 hr at room temperature. Incubation volumes were 100 $\mu\text{l/well}$ except for the blocking steps which contained 150 $\mu\text{l/well}$. scFvs and detection antibodies were applied in 1% skimmed dried milk in TBSM. In experiments testing the metal ion dependence of the anti- $\alpha\nu\beta 6$ scFvs, the diluent was TBS containing 5 mM EDTA, pH 7.5, and all washing steps included 5 mM EDTA.

Inhibition of binding of B6-1 to immobilized $\alpha\nu\beta 6$ by ELISA

Ninety-six-well plates were coated with 3 $\mu\text{g/ml}$ of $\alpha\nu\beta 6$, washed and blocked. The wells were subsequently incubated with 100 nM of anti- $\alpha\nu\beta 6$, anti- $\alpha\nu\beta 3$ or 20-mer VP1 peptide²⁴ for 15 min, followed by the addition of 50 ng (in 1 μl) of B6-1 and incubation for a further 30 min. B6-1 and MFE-23 were used without inhibitors as positive and negative controls, respectively. The secondary and tertiary antibodies were rabbit anti-MFE-23 IgG and HRP-conjugated goat anti-rabbit IgG, respectively. Washing, blocking and detection of bound B6-1 were performed as described in '*Binding of MFE-23 CDR-H3 variants to immobilized $\alpha\nu\beta 6$ and $\alpha\nu\beta 3$ by ELISA*'.

Binding of scFvs to immobilized CEA by ELISA

Plates were coated with 1 $\mu\text{g/ml}$ CEA in PBS, washed twice with PBS on an automatic plate washer (Thermo Labsystems) and blocked with 5% skimmed dried milk in PBS. B6-1, B6-2 or MFE-23 was added to the wells in triplicate, followed by: automatic washing as above, incubation with rabbit anti-MFE-23 IgG (1:1000 dilution), automatic washing with 0.1% Tween-20/PBS (x2) and H_2O (x4), incubation with HRP-conjugated goat anti-rabbit IgG (1:1000 dilution) and automatic washing with 0.1% Tween-20/PBS (x2) and H_2O (x4). Binding was detected with *o*-phenylenediamine dihydrochloride, and absorbance read at 490 nm. Plates, incubation volumes and absorbance readings were as described in '*Binding of MFE-23 CDR-H3 variants to immobilized $\alpha\nu\beta 6$ and $\alpha\nu\beta 3$ by ELISA*'. scFvs and subsequent antibodies were applied in 1% skimmed dried milk in PBS.

Flow cytometric analysis of scFv binding to CEA-expressing cells

LS174T cells were trypsinized. On average, 5×10^5 cells were incubated with 50 $\mu\text{g/ml}$ of B6-1, B6-2 or MFE-23 and washed with PBS. Binding was detected by incubation with rabbit anti-MFE-23 IgG (1:100 dilution), followed by: washing with PBS, incubation with 1 μg of R-Phycoerythrin (R-PE)-conjugated goat anti-rabbit IgG (Invitrogen) and washing with PBS. All incubation steps were carried out for 60 min at 4 °C in 100 μl PBS containing 0.1% (w/v) bovine serum albumin (BSA) and 0.1 % (w/v) sodium azide. In control experiments, the rabbit anti-MFE-23 IgG was omitted. Cells were fixed (IntraStain kit, DakoCytomation) and analyzed by flow cytometry on a FACSCalibur™ cytometer (Becton Dickinson).

Flow cytometric analysis of scFv binding to $\alpha\text{v}\beta\text{6}$ -expressing cells

A375P β6 and A375Ppuro cells were washed once in Dulbecco's modified Eagle's medium (DMEM) supplemented with 0.1% (w/v) BSA and 0.1% (w/v) sodium azide (DMEM 0.1/0.1). Cells ($\sim 2 \times 10^5$) were then transferred to individual wells of V-bottomed 96-well plates and mixed with 50 μl of B6-1 or MFE-23 at various concentrations or 10D5 (Chemicon International) at 10 $\mu\text{g/ml}$ and incubated at 4 °C for 60 min. Secondary and tertiary antibodies for B6-1 were mouse Tetra-His antibody (Qiagen) diluted 1:1000 in DMEM 0.1/0.1 (incubated 35 min at 4°C) and Alexa Fluor 488®-conjugated goat anti-mouse IgG (Invitrogen) diluted 1:200 in DMEM 0.1/0.1 (incubated 30 min at 4°C), respectively. The secondary antibody for 10D5 was Alexa Fluor 488®-conjugated goat anti-mouse IgG and used as above. Washes between incubations were carried out two times with 150 μl DMEM 0.1/0.1 and three times after the final incubation step. Binding of B6-2 and MFE-23 (at 50 $\mu\text{g/ml}$) to these cells shown in Fig. 5d was detected with rabbit anti-MFE-23 IgG (1:1000 dilution) followed by R-PE-conjugated goat anti-rabbit IgG (1 $\mu\text{g/ml}$). For analysis on a LSR-1 FACS flow cytometer (Becton Dickinson) using CellQuest software, cells were transferred to 5 ml centrifuge tubes (BD Falcon 352054, supplied by VWR).

Flow cytometric characterisation of integrin expression

A375Ppuro and A375P β6 cells were trypsinized, resuspended in DMEM 0.1/0.1 to $\sim 2 \times 10^5$ cells/50 μl and mixed with 50 μl of anti-integrin antibodies (at 10 $\mu\text{g/ml}$). After 45 min at 4 °C, the cells were washed twice with DMEM 0.1/0.1 and bound antibodies were detected with 50 μl of 1:200 dilutions of Alexa Fluor 488®-conjugated goat anti-mouse IgG antibodies (Invitrogen) for 30 min at 4 °C. After two washes, samples were analyzed by flow cytometry as described in '*Flow cytometric analysis of scFv binding to $\alpha\text{v}\beta\text{6}$ -expressing cells*'. Negative controls received similar concentrations of mouse IgG (DakoCytomation).

Flow cytometric analysis of inhibition of binding of B6-1 to $\alpha\text{v}\beta\text{6}$ -expressing cells

A375P β6 cells were trypsinised, re-suspended in DMEM 0.1/0.1 to $\sim 5 \times 10^5$ cells/100 μl and incubated with various concentrations of anti- $\alpha\text{v}\beta\text{6}$ or anti- $\alpha\text{v}\beta\text{3}$ for 15 min at 4 °C. Fifty nanograms of B6-1 (in 1 μl PBS) was subsequently added, and the cells were incubated for a further 30 min at 4 °C. Bound B6-1 was detected with rabbit anti-MFE-23 IgG (1:1000 dilution) followed by R-PE-conjugated goat anti-rabbit IgG (1 $\mu\text{g/ml}$). Positive control experiments that used B6-1 and negative experiments that used MFE-23 only (both at 50 ng/100 μl) were also performed. Detection antibodies were incubated for 45 min at 4 °C, and all incubations were followed by washing with DMEM 0.1/0.1. Cells were fixed and analyzed as described in '*Flow cytometric analysis of scFv binding to CEA-expressing cells*'.

Immunofluorescence microscopy of internalized B6-2

A375Pβ6 and A375Ppuro cells ($\sim 2 \times 10^5$) were trypsinized, re-suspended in DMEM containing L-glutamine and supplemented with 10% heat-inactivated fetal bovine serum, seeded on to glass coverslips in 2 ml of the above media and incubated for 48 h at 37 °C. The media were exchanged with DMEM containing 1% heat-inactivated fetal bovine serum (DMEM 1) and 50 μg/ml B6-2 and incubated for 0 min, 10 min, 30 min, 1 h or 3 h at 37 °C. In a further set of experiments, cells were first pre-incubated at 4 °C for 1 h in DMEM 1 containing 50 μg/ml of B6-2, followed by removal of the scFv-containing supernatant and subsequent incubation in DMEM 1 at 37 °C for the same times as above. After incubation, the cells on the coverslips were washed twice in PBS, containing 2 mM Ca²⁺ and 1 mM Mg²⁺, followed by: fixation in 4% paraformaldehyde/PBS for 20 min on ice, washing and incubation with 10 mM ammonium chloride for 10 min at room temperature, permeabilization with 0.1% Triton X-100 for 5 min, blocking with 3% (w/v) BSA/PBS for 20 min at room temperature, staining with 10 μg/ml rabbit anti-mouse IgG (Jackson Immuno Research) in 1% (w/v) BSA/PBS and staining with Alexa Fluor 546® labeled goat anti-rabbit IgG (Invitrogen), containing Hoechst trihydrochloride (1:5000) in 1% (w/v) BSA/PBS. Coverslips were lastly mounted on slides using ProLong Gold antifade (Invitrogen) and examined using a Zeiss LSM 510 Meta laser scanning confocal microscope (Zeiss).

Cell migration assay

Haptotactic cell migration assays were performed using matrix coated polycarbonate filters (8 μm pore size, Transwell®, Becton Dickinson). The membrane undersurface was coated with LAP (0.5 μg/ml) in α-MEM for 1 h at 37 °C and blocked with migration buffer (0.1% BSA in α-MEM) for 30 min at 37 °C. For blocking experiments, VB6 cells were incubated for 60 min at 4 °C prior to seeding with B6-1, B6-2, MFE-23 (all at 50 μg/ml) or 10D5 antibody (at 10 μg/ml, Chemicon International) (Fig. 4a), with B6-1 at various concentrations (Fig. 4b) and with B6-1, B6-2, MFE-23 (all at 100nM) and the 20-mer VP1 peptide at various concentrations (Fig. 4c). The lower chamber was filled with 500 μl of migration buffer, following which cells were plated in the upper chamber of quadruplicate wells, at a density of 5×10^4 in 50 μl of migration buffer, and incubated at 37 °C for 20 h. Following incubation, the cells in the lower chamber (including those attached to the undersurface of the membrane) were trypsinized and counted on a Casy 1 counter (Sharfe System GmbH).

FT-IR spectroscopy

B6-2 at 0.47 mg/ml, MFE-23 at 0.59 mg/ml and PBS control were dialyzed into 20 mM Phosphate buffer, pH7.5 and subsequently lyophilized. B6-2 and MFE-23 were dissolved in ²H₂O to a final concentration of 10 mg/ml and control at an equivalent volume. Eight microliters of each protein and control were used for analysis. For denaturation experiments, the protein was exposed to temperatures from 25 °C to 85 °C in steps of 2-5 °C. A total of 200 scans was acquired at each temperature for the denaturation measurements, whereas for comparison of B6-2 to MFE-23 secondary structural elements, 1000 scans were acquired at 30 °C each. FT-IR spectra were recorded and analyzed as described previously.³³

Inhibition of cell adhesion assay

The ability of modified and unmodified scFv antibodies to inhibit the αvβ6-specific adhesion of [⁵¹Cr]3T3β6.19 fibroblast cells to LAP was performed as described previously.

24

Supplementary Material

Refer to Web version on PubMed Central for supplementary material.

Acknowledgments

This work was supported by Cancer Research UK grant C34/A5149 and the UCL Cancer Institute Research Trust.

Abbreviations used

BSA	bovine serum albumin
CDR	complementary-determining region
CEA	carcinoembryonic antigen
DMEM	Dulbecco's modified Eagle's medium
FMDV	foot-and-mouth disease virus
HRP	horseradish peroxidase
IgG	immunoglobulin G
IMAC	immobilized metal-affinity chromatography
LAP	latency associated protein
PBS	phosphate-buffered saline
R-PE	R-phycoerythrin
RGD	arginine-glycine-aspartic acid
scFv	single-chain Fv
shMFE	stabilized humanized MFE-23
TBS	Tris-buffered saline
TGF	transforming growth factor
TNF	tumor necrosis factor
V_H	variable heavy chain
VL	variable light chain
VP1	viral protein 1

References

1. Hynes RO. Integrins: bidirectional, allosteric signaling machines. *Cell*. 2002; 110:673–687. [PubMed: 12297042]
2. Breuss JM, Gallo J, DeLisser HM, Klimanskaya IV, Folkesson HG, Pittet JF, Nishimura SL, Aldape K, Landers DV, Carpenter W, Gillett N, Sheppard D, Matthy MA, Albelda SM, Kramer RH, Pytela R. Expression of the beta 6 integrin subunit in development, neoplasia and tissue repair suggests a role in epithelial remodeling. *J. Cell Sci*. 1995; 108:2241–2251. [PubMed: 7673344]
3. Ruoslahti E. Integrins. *J. Clin. Invest*. 1991; 87:1–5. [PubMed: 1985087]
4. Giancotti FG, Mainiero F. Integrin-mediated adhesion and signaling in tumorigenesis. *Biochim. Biophys. Acta*. 1994; 1198:47–64. [PubMed: 8199195]
5. Thomas GJ, Nystrom ML, Marshall JF. Alphavbeta6 integrin in wound healing and cancer of the oral cavity. *J. Oral Pathol. Med*. 2006; 35:1–10. [PubMed: 16393247]

6. Arihiro K, Kaneko M, Fujii S, Inai K, Yokosaki Y. Significance of alpha 9 beta 1 and alpha v beta 6 integrin expression in breast carcinoma. *Breast Cancer*. 2000; 7:19–26. [PubMed: 11029766]
7. Sipos B, Hahn D, Carceller A, Piulats J, Hedderich J, Kalthoff H, Goodman SL, Kosmahl M, Kloppel G. Immunohistochemical screening for beta6-integrin subunit expression in adenocarcinomas using a novel monoclonal antibody reveals strong up-regulation in pancreatic ductal adenocarcinomas in vivo and in vitro. *Histopathology*. 2004; 45:226–236. [PubMed: 15330800]
8. Ahmed N, Pansino F, Clyde R, Murthi P, Quinn MA, Rice GE, Agrez MV, Mok S, Baker MS. Overexpression of alpha(v)beta6 integrin in serous epithelial ovarian cancer regulates extracellular matrix degradation via the plasminogen activation cascade. *Carcinogenesis*. 2002; 23:237–244. [PubMed: 11872628]
9. Munger JS, Huang X, Kawakatsu H, Griffiths MJ, Dalton SL, Wu J, Pittet JF, Kaminski N, Garat C, Matthay MA, Rifkin DB, Sheppard D. The integrin alpha v beta 6 binds and activates latent TGF beta 1: a mechanism for regulating pulmonary inflammation and fibrosis. *Cell*. 1999; 96:319–328. [PubMed: 10025398]
10. Bates RC, Bellovin DI, Brown C, Maynard E, Wu B, Kawakatsu H, Sheppard D, Oettgen P, Mercurio AM. Transcriptional activation of integrin beta6 during the epithelial-mesenchymal transition defines a novel prognostic indicator of aggressive colon carcinoma. *J. Clin. Invest.* 2005; 115:339–347. [PubMed: 15668738]
11. Hazelbag S, Kenter GG, Gorter A, Dreef EJ, Koopman LA, Violette SM, Weinreb PH, Fleuren GJ. Overexpression of the alpha v beta 6 integrin in cervical squamous cell carcinoma is a prognostic factor for decreased survival. *J. Pathol.* 2007; 212:316–324. [PubMed: 17503414]
12. Elayadi AN, Samli KN, Prudkin L, Liu YH, Bian A, Xie XJ, Wistuba II, Roth JA, McGuire MJ, Brown KC. A peptide selected by biopanning identifies the integrin alphavbeta6 as a prognostic biomarker for nonsmall cell lung cancer. *Cancer Res.* 2007; 67:5889–5895. [PubMed: 17575158]
13. Ramos DM, But M, Regezi J, Schmidt BL, Atakilit A, Dang D, Ellis D, Jordan R, Li X. Expression of integrin b6 enhances invasive behavior in oral squamous cell carcinoma. *Matrix Biology*. 2002; 21:297–307. [PubMed: 12009335]
14. Adams GP, Weiner LM. Monoclonal antibody therapy of cancer. *Nat. Biotechnol.* 2005; 23:1147–1157.1. [PubMed: 16151408]
15. Holliger P, Hudson PJ. Engineered antibody fragments and the rise of single domains. *Nat. Biotechnol.* 2005; 23:1126–1136. [PubMed: 16151406]
16. Wu AM, Senter PD. Arming antibodies: prospects and challenges for immunoconjugates. *Nat. Biotechnol.* 2005; 23:1137–1146. [PubMed: 16151407]
17. Logan D, Abu-Ghazaleh R, Blakemore W, Curry S, Jackson T, King A, Lea S, Lewis R, Newman J, Parry N, Rowlands D, Stuart D, Fry E. Structure of a major immunogenic site on foot-and-mouth disease virus. *Nature*. 1993; 362:566–568. [PubMed: 8385272]
18. Monaghan P, Gold S, Simpson J, Zhang Z, Weinreb PH, Violette SM, Alexandersen S, Jackson T. The alpha(v)beta6 integrin receptor for Foot-and-mouth disease virus is expressed constitutively on the epithelial cells targeted in cattle. *J. Gen. Virol.* 2005; 86:2769–2780. [PubMed: 16186231]
19. Brown JK, McAleese SM, Thornton EM, Pate JA, Schock A, Macrae AI, Scott PR, Miller HR, Collie DD. Integrin-alphavbeta6, a putative receptor for foot-and-mouth disease virus, is constitutively expressed in ruminant airways. *J. Histochem. Cytochem.* 2006; 54:807–816. [PubMed: 16517977]
20. Jackson T, King AM, Stuart DI, Fry E. Structure and receptor binding. *Virus Res.* 2003; 91:33–46. [PubMed: 12527436]
21. Burman A, Clark S, Abrescia NG, Fry EE, Stuart DI, Jackson T. Specificity of the VP1 GH loop of Foot-and-Mouth Disease virus for alphav integrins. *J. Virol.* 2006; 80:9798–9810. [PubMed: 16973584]
22. Ludbrook SB, Barry ST, Delves CJ, Horgan CM. The integrin alphavbeta3 is a receptor for the latency-associated peptides of transforming growth factors beta1 and beta3. *Biochem. J.* 2003; 369:311–318. [PubMed: 12358597]

23. Duque H, LaRocco M, Golde WT, Baxt B. Interactions of foot-and-mouth disease virus with soluble bovine alphaVbeta3 and alphaVbeta6 integrins. *J. Virol.* 2004; 78:9773–9781. [PubMed: 15331710]
24. Dicara D, Rapisarda C, Sutcliffe JL, Violette SM, Weinreb PH, Hart IR, Howard MJ, Marshall JF. Structure-function analysis of RGD-helix motifs in alpha vbeta 6 integrin ligands. *J. Biol. Chem.* 2007;1.
25. Boehm MK, Corper AL, Wan T, Sohi MK, Sutton BJ, Thornton JD, Keep PA, Chester KA, Begent RH, Perkins SJ. Crystal structure of the anti-(carcinoembryonic antigen) single-chain Fv antibody MFE-23 and a model for antigen binding based on intermolecular contacts. *Biochem. J.* 2000; 346:519–528. [PubMed: 10677374]
26. Chester KA, Begent RH, Robson L, Keep P, Pedley RB, Boden JA, Boxer G, Green A, Winter G, Cochet O, Hawkins RE. Phage libraries for generation of clinically useful antibodies. *Lancet.* 1994; 343:455–456. [PubMed: 7905958]
27. Begent RH, Verhaar MJ, Chester KA, Casey JL, Green AJ, Napier MP, Hope-Stone LD, Cushen N, Keep PA, Johnson CJ, Hawkins RE, Hilson AJ, Robson L. Clinical evidence of efficient tumor targeting based on single-chain Fv antibody selected from a combinatorial library. *Nat. Med.* 1996; 2:979–984. [PubMed: 8782454]
28. Mayer A, Tsiompanou E, O'Malley D, Boxer GM, Bhatia J, Flynn AA, Chester KA, Davidson BR, Lewis AA, Winslet MC, Dhillon AP, Hilson AJ, Begent RH. Radioimmunoguided surgery in colorectal cancer using a genetically engineered anti-CEA single-chain Fv antibody. *Clin. Cancer Res.* 2000; 6:1711–1719. [PubMed: 10815889]
29. Chester KA, Bhatia J, Boxer G, Cooke SP, Flynn AA, Huhlov A, Mayer A, Pedley RB, Robson L, Sharma SK, Spencer DI, Begent RH. Clinical applications of phage-derived sFvs and sFv fusion proteins. *Dis. Markers.* 2000; 16:53–62. [PubMed: 11360829]
30. Chester KA, Mayer A, Bhatia J, Robson L, Spencer DI, Cooke SP, Flynn AA, Sharma SK, Boxer G, Pedley RB, Begent RH. Recombinant anti-carcinoembryonic antigen antibodies for targeting cancer. *Cancer Chemother. Pharmacol.* 2000; 46:S8–12. [PubMed: 10950140]
31. Read DA, Chester KA, Keep PA, Begent RHJ, Pedersen JT, Rees AR. *Br. J. Cancer.* 1995; 71:57.
32. Thomas GJ, Hart IR, Speight PM, Marshall JF. Binding of TGF-beta1 latency-associated peptide (LAP) to alpha(v)beta6 integrin modulates behaviour of squamous carcinoma cells. *Br. J. Cancer.* 2002; 87:859–867. [PubMed: 12373600]
33. Lee YC, Boehm MK, Chester KA, Begent RH, Perkins SJ. Reversible dimer formation and stability of the anti-tumour single-chain Fv antibody MFE-23 by neutron scattering, analytical ultracentrifugation, and NMR and FT-IR spectroscopy. *J. Mol. Biol.* 2002; 320:107–127. [PubMed: 12079338]
34. Graff CP, Chester K, Begent R, Wittrup KD. Directed evolution of an anti-carcinoembryonic antigen scFv with a 4-day monovalent dissociation half-time at 37 degrees C. *Protein Eng Des Sel.* 2004; 17:293–304. [PubMed: 15115853]
35. Jackson T, Sheppard D, Denyer M, Blakemore W, King AM. The epithelial integrin alphavbeta6 is a receptor for foot-and-mouth disease virus. *J Virol.* 2000; 74:4949–4956. [PubMed: 10799568]
36. Boehm MK, Perkins SJ. Structural models for carcinoembryonic antigen and its complex with the single-chain Fv antibody molecule MFE23. *FEBS Lett.* 2000; 475:11–16. [PubMed: 10854848]
37. Frederickson S, Renshaw MW, Lin B, Smith LM, Calveley P, Springhorn JP, Johnson K, Wang Y, Su X, Shen Y, Bowdish KS. A rationally designed agonist antibody fragment that functionally mimics thrombopoietin. *Proc. Natl. Acad. Sci. U. S. A.* 2006; 103:14307–14312. [PubMed: 16973749]
38. Kohler G, Milstein C. Continuous cultures of fused cells secreting antibody of predefined specificity. *Nature.* 1975; 256:495–497. [PubMed: 1172191]
39. Winter G, Griffiths AD, Hawkins RE, Hoogenboom HR. Making antibodies by phage display technology. *Annu. Rev. Immunol.* 1994; 12:433–455. [PubMed: 8011287]
40. McLane KE, Burton DR, Ghazal P. Transplantation of a 17-amino acid alpha-helical DNA-binding domain into an antibody molecule confers sequence-dependent DNA recognition. *Proc. Natl. Acad. Sci. U. S. A.* 1995; 92:5214–5218. [PubMed: 7761476]

41. Moroncini G, Kanu N, Solfrosi L, Abalos G, Telling GC, Head M, Ironside J, Brockes JP, Burton DR, Williamson RA. Motif-grafted antibodies containing the replicative interface of cellular PrP are specific for PrPSc. *Proc. Natl. Acad. Sci. U. S. A.* 2004; 101:10404–10409. [PubMed: 15240877]
42. Qin W, Feng J, Li Y, Lin Z, Shen B. A novel domain antibody rationally designed against TNF- α using variable region of human heavy chain antibody as scaffolds to display antagonistic peptides. *Mol. Immunol.* 2007; 44:2355–2361. [PubMed: 17125837]
43. Main AL, Harvey TS, Baron M, Boyd J, Campbell ID. The three-dimensional structure of the tenth type III module of fibronectin: an insight into RGD-mediated interactions. *Cell.* 1992; 71:671–678. [PubMed: 1423622]
44. Lanza P, Felding-Habermann B, Ruggeri ZM, Zanetti M, Billetta R. Selective interaction of a conformationally-constrained Arg-Gly-Asp (RGD) motif with the integrin receptor α v β 3 expressed on human tumor cells. *Blood Cells Mol. Dis.* 1997; 23:230–241. [PubMed: 9268674]
45. Lanza P, Billetta R, Antonenko S, Zanetti M. Active immunity against the CD4 receptor by using an antibody antigenized with residues 41-55 of the first extracellular domain. *Proc. Natl. Acad. Sci. U. S. A.* 1993; 90:11683–11687. [PubMed: 8265609]
46. Hoogenboom HR. Selecting and screening recombinant antibody libraries. *Nat. Biotechnol.* 2005; 23:1105–1116. [PubMed: 16151404]
47. Thomas GJ, Lewis MP, Whawell SA, Russell A, Sheppard D, Hart IR, Speight PM, Marshall JF. Expression of the α v β 6 integrin promotes migration and invasion in squamous carcinoma cells. *J. Invest Dermatol.* 2001; 117:67–73. [PubMed: 11442751]
48. Hawkins RE, Zhu D, Ovecká M, Winter G, Hamblin TJ, Long A, Stevenson FK. Idiotypic vaccination against human B-cell lymphoma. Rescue of variable region gene sequences from biopsy material for assembly as single-chain Fv personal vaccines. *Blood.* 1994; 83:3279–3288. [PubMed: 8193363]
49. Tolner B, Smith L, Begent RH, Chester KA. Production of recombinant protein in *Pichia pastoris* by fermentation. *Nat. Protoc.* 2006; 1:1006–1021. [PubMed: 17406338]
50. Tolner B, Smith L, Begent RH, Chester KA. Expanded-bed adsorption immobilized-metal affinity chromatography. *Nat. Protoc.* 2006; 1:1213–1222. [PubMed: 17406404]
51. Weinacker A, Chen A, Agrez M, Cone RI, Nishimura S, Wayner E, Pytela R, Sheppard D. Role of the integrin α v β 6 in cell attachment to fibronectin. Heterologous expression of intact and secreted forms of the receptor. *J. Biol. Chem.* 1994; 269:6940–6948. [PubMed: 8120056]

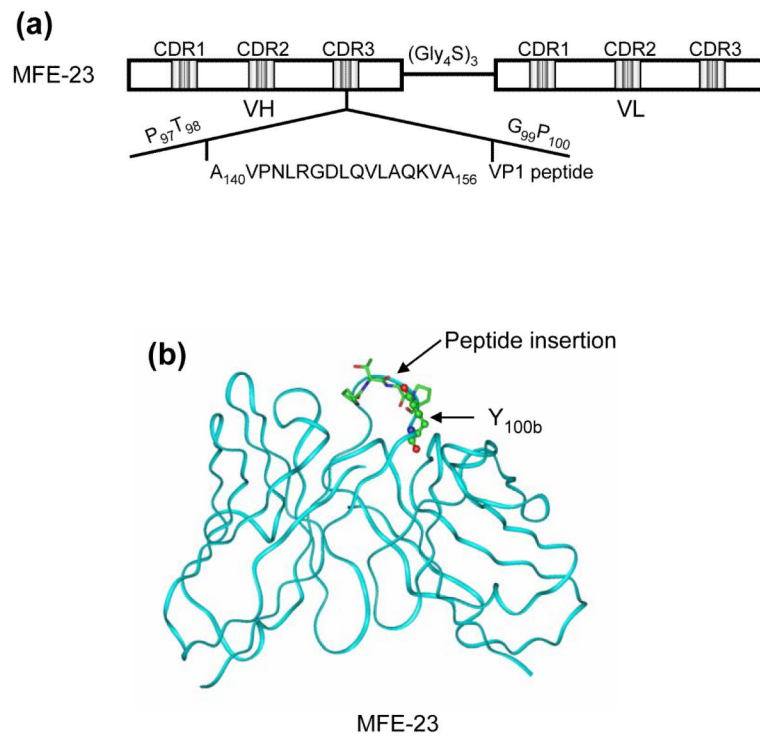


Fig. 1. Schematic presentation of the construction of B6-1 and B6-2. (a) Insertion of the RGD containing peptide sequence of VP1 (A₁₄₀ to A₁₅₆)₁₇ into the CDR3 loop (between T₉₈ and G₉₉) of the VH chain of MFE-23 that gives B6-1. (b) Ribbon diagram of the x-ray structure of MFE-23.25 CDR3 loop residues P₉₇ to P₁₀₀ of the VH chain of MFE-23 are shown in stick presentation, and the site of peptide insertion in MFE-23 is indicated. Y_{100b} that was mutated to P_{100b} to give B6-2 is shown in ball-and-stick presentation.

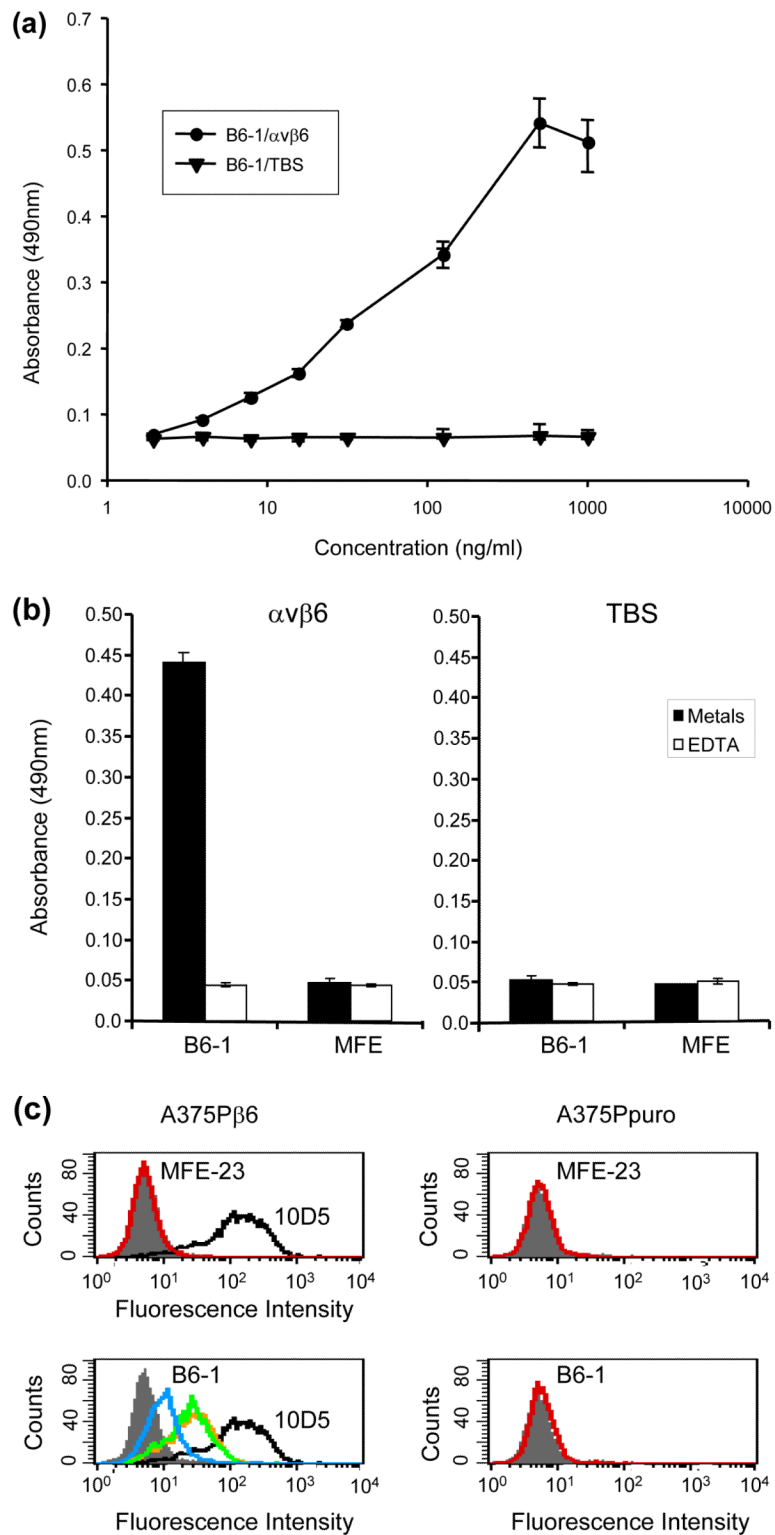


Fig. 2. Interactions of B6-1 with α v β 6. (a) Graph showing concentration-dependent binding of B6-1 to immobilized α v β 6 in ELISA. B6-1 (various concentrations) was applied to immobilized α v β 6 or control Tris-buffered (TBS) wells. Binding was detected with rabbit

anti-MFE-23 IgG followed by goat HRP-linked secondary anti-rabbit IgG antibody. (b) Graph showing cation-dependent binding of B6-1 to immobilized $\alpha v \beta 6$ in ELISA. B6-1 or MFE (both at 0.5 $\mu\text{g/ml}$) was applied to immobilized $\alpha v \beta 6$ or control Tris-buffered (TBS) wells either in the presence of Ca^{2+} , Mg^{2+} and Mn^{2+} (cations) or in the presence of EDTA (5 mM). Binding was detected as described in (a). (c) Flow cytometry analyses show concentration-dependent binding of B6-1 to $\alpha v \beta 6$ on cells. MFE-23 or B6-1 was allowed to bind to $\alpha v \beta 6$ -expressing (A375P $\beta 6$) and non-expressing (A375Ppuro) cells. 10D5 murine anti- $\alpha v \beta 6$, used at 10 $\mu\text{g/ml}$ as a positive control for $\beta 6$ -transfected cells, is shown in black in both left panels. Bound scFvs were detected with mouse anti-Tetra-His IgG followed by Alexa Fluor 488®-conjugated anti-mouse IgG. Top left panel shows A375P $\beta 6$, and top right panel shows A375Ppuro cells and MFE-23 at 50 $\mu\text{g/ml}$ (red); bottom left panel shows A375P $\beta 6$ cells and B6-1 at 5 $\mu\text{g/ml}$ (orange), 0.5 $\mu\text{g/ml}$ (green) and 0.05 $\mu\text{g/ml}$ (blue). The 50 $\mu\text{g/ml}$ concentration (not shown) had a shift in fluorescence intensity identical with that for the 5 $\mu\text{g/ml}$ concentration; bottom right panel shows A375Ppuro cells, B6-1 at 50 $\mu\text{g/ml}$ (red). Cells treated with mouse anti-Tetra-His IgG and Alexa Fluor488®-conjugated anti-mouse IgG only (omission controls) are shown in grey. The data represent the mean of triplicate measurements, and error bars represent the standard deviation at each data point (a and b).

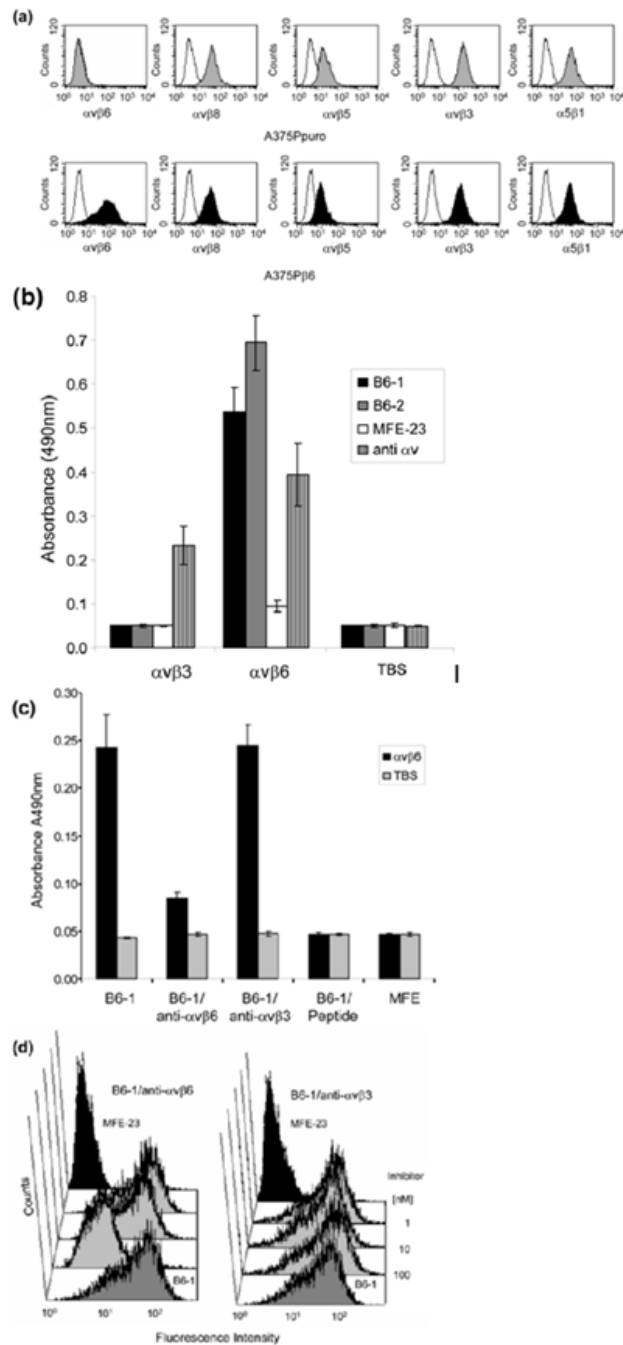


Fig. 3. Specificity of B6-1 for $\alpha v \beta 6$. (a) Flow cytometry analyses show that B6-1 did not bind to A375Ppuro cells even though they express the RGD-directed integrins $\alpha v \beta 8$, $\alpha v \beta 5$, $\alpha v \beta 3$ and $\alpha 5 \beta 1$ as detected by the same anti-integrin antibodies, in the same conditions, on both cell lines. Negative controls (white histograms) were incubated with Alexa Fluor 488-conjugated goat anti-mouse IgG only. (b) Graph showing that B6-1 did bind to immobilized $\alpha v \beta 6$ and not to $\alpha v \beta 3$ in ELISA. MFE-23 did not bind to either of these integrins. Binding of B6-1, B6-2 and MFE-23 (all at 5 $\mu\text{g/ml}$) to immobilized $\alpha v \beta 3$ or $\alpha v \beta 6$ wells was detected with rabbit anti-MFE-23 IgG followed by goat HRP-labeled anti-rabbit IgG antibodies. Wells were also incubated with mouse anti- αv , followed by sheep HRP-labeled

anti-mouse IgG, to detect whether the integrin was immobilized,. (c) Graph showing that binding of B6-1 [50 ng/ml, 1.75 nM] to immobilized $\alpha v\beta 6$ was inhibited by anti- $\alpha v\beta 6$ (at 100 nM) and by the 20-mer VP1 peptide24 (at 100 nM) but not by a function-blocking anti- $\alpha v\beta 3$ antibody (at 100 nM). B6-1 and MFE-23 used on its own were included as positive and negative controls, respectively. Binding was detected as described in Fig. 2a. (d) Flow cytometry demonstrates that binding of B6-1 (at 500 ng/ml, 17.5 nM) to $\alpha v\beta 6$ -expressing A375P $\beta 6$ cells was inhibited by anti- $\alpha v\beta 6$ antibody (at 100 nM) (left panel, second trace from front), whereas the same concentration of anti- $\alpha v\beta 3$ had no effect (right panel, second trace from front). B6-1 (left and right panels, first traces from front) and MFE-23 (left and right panels, last traces), both at 500 ng/ml, were included as positive and negative controls, respectively. Binding was revealed with rabbit anti-MFE-23 IgG followed by R-PE-labeled goat anti rabbit IgG. The data represent the mean of triplicate measurements and error bars represent the standard deviation at each data point (b and c).

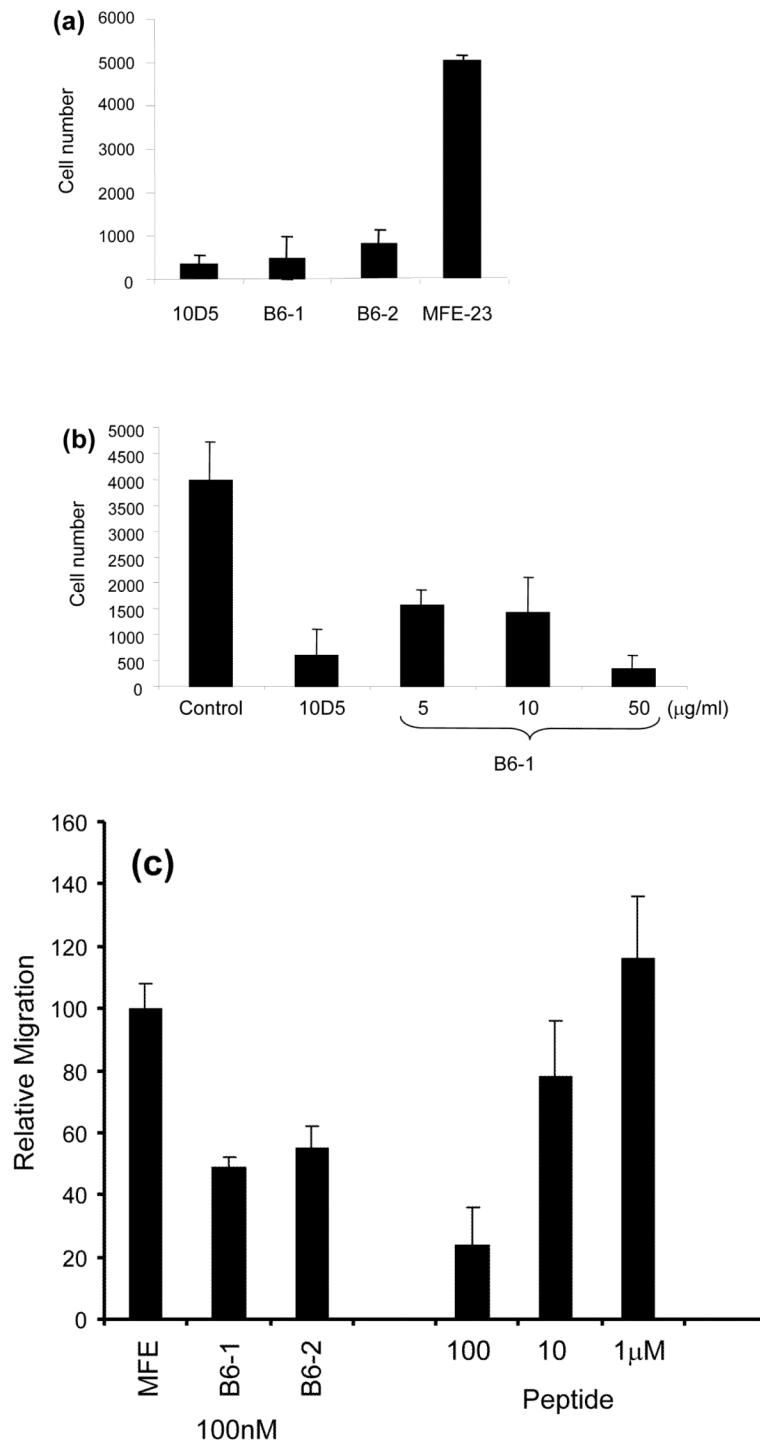


Fig. 4. Inhibition of cell migration by B6-1 and B6-2. (a-c) Charts showing that B6-1 and B6-2 blocked the migration of $\alpha\beta6$ -expressing cells towards LAP. VB6 cells were allowed to migrate through LAP-coated Transwell® filters. Inhibition of cell migration was observed for B6-1, B6-2 (both at 50 µg/ml) and 10D5 in (a), in a concentration-dependent manner for B6-1 in (b) and B6-1 and B6-2 (at 100 nM) and the 20-mer VP1 peptide, A20FMDV224 (at 1, 10 and 100 µM) in (c). The control antibody W6/32 (anti-major histocompatibility

complex class 1) and 10D5 were used at 1:100 and 10 $\mu\text{g/ml}$, respectively. The data represent the mean of quadruplet measurements and error bars represent the standard deviation at each data point (a-c).

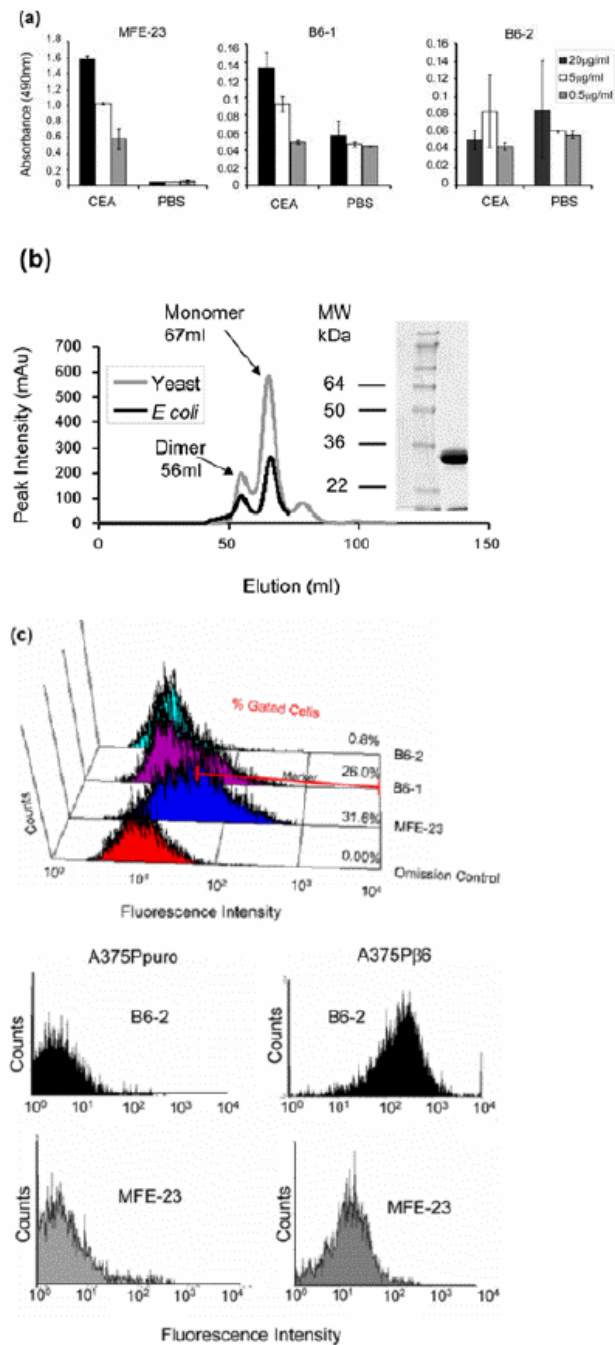


Fig. 5. Production and characterization of the Y100bP mutant B6-2. (a) Chart showing concentration-dependent residual binding of B6-1 to immobilized CEA, which was eliminated in the Y100bP mutant B6-2. B6-1 (middle panel), B6-2 (right panel) and MFE-23 (left panel), at three different concentrations, were added to immobilized CEA and PBS wells. Binding was detected with rabbit anti-MFE-23 IgG followed by goat HRP-labeled anti-rabbit IgG. The data represent the mean of triplicate measurements and error bars represent the standard deviation at each data point. (b) Size-exclusion chromatographic profiles show that *E. coli* and *P. pastoris*-expressed B6-2 was superimposable and gave monomeric (67 ml) and dimeric (56 ml) forms. This is consistent with MFE-23, which also

gave monomeric (68 ml) and dimeric (58 ml) forms (data not shown). The monomeric fraction of B6-2 was used for all experiments. Twelve percent Tri-glycine reducing SDS-PAGE shows the monomeric (M) fraction of the *P. pastoris*-expressed B6-2. (c) Flow cytometry analyses show that B6-1's binding to CEA expressing LS174T cells was eliminated in the Y100bP mutant. LS174T cells were incubated with B6-1, B6-2 or MFE-23 (all at 50 $\mu\text{g/ml}$). Binding was detected with rabbit anti-MFE-23 IgG followed by R-PE-labeled goat anti-rabbit IgG. In the omission control shown, cells were incubated with MFE-23 at 50 $\mu\text{g/ml}$ followed by R-PE-labeled goat anti-rabbit IgG. Results are representative of three independent experiments. Percentages of gated cells at fluorescence intensities of $7 \times 10^1 - 10^4$ (as indicated) are mean values from three separate experiments of which the mean control values had been subtracted. (d) Flow cytometry analyses show that B6-2 bound to A373P β 6 cells but not to A375puro cells. Cells were incubated with MFE or B6-2 (at 50 $\mu\text{g/ml}$). Binding was detected as described under (c).

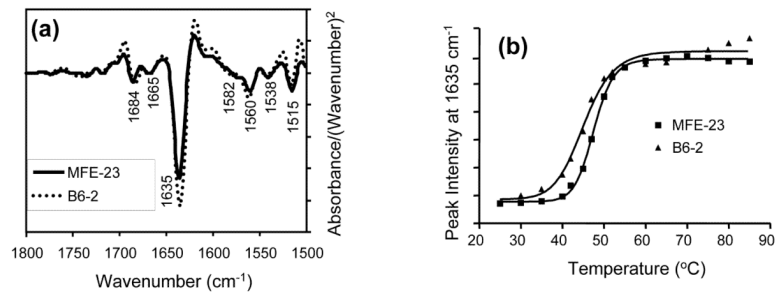


Fig. 6. Stability of B6-2. (a and b) FT-IR spectra show that B6-2 maintained the secondary structural elements and had a similar midpoint of denaturation as the parent MFE-23. (a) Second derivative FT-IR spectra of B6-2 and MFE-23 were obtained from the absorbance spectra recorded at 30 °C after buffer control subtraction. (b) For the denaturation curve, both proteins were heated from 25 to 85 °C and the FT-IR spectra were measured. The midpoints of denaturation were obtained from fitting of the peak intensity at 1635 cm⁻¹ of the second-derivative spectra to a sigmoidal curve as 47 °C for MFE-23 and 45 °C for B6-2.

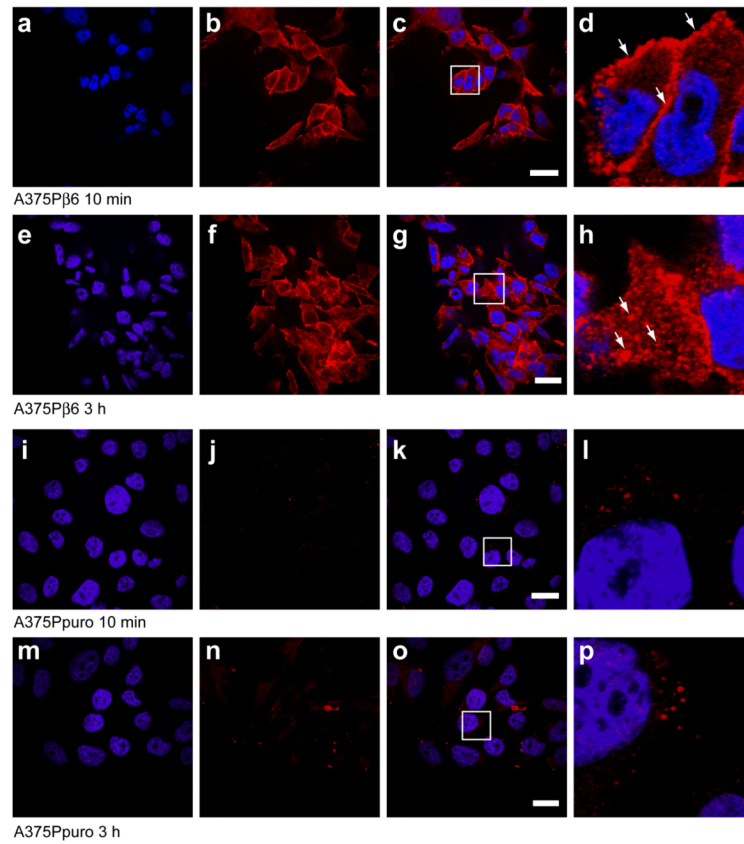


Fig. 7. B6-2 is internalized by $\alpha v \beta 6$ -expressing cells. Indirect immunofluorescence confocal microscopy analyses show detection of cell surface-bound and internalized B6-2. $\alpha v \beta 6$ -expressing (A375P $\beta 6$, a-h) and non-expressing (A375Ppuro, i-p) cells were incubated with B6-2 for 1hr at 4°C, free scFv was subsequently removed and the cells were incubated at 37 °C for the times indicated. Zoom boxes show the predominant plasma membrane pattern of staining at 10 minutes (d) and internalized vesicular staining at 3 h (h). B6-2 was detected using rabbit anti-mouse IgG followed by Alexa Fluor® 546-labeled goat anti-rabbit IgG (red). Cells were also counterstained with Hoechst 33245 (blue). Scale bars 20 mm.

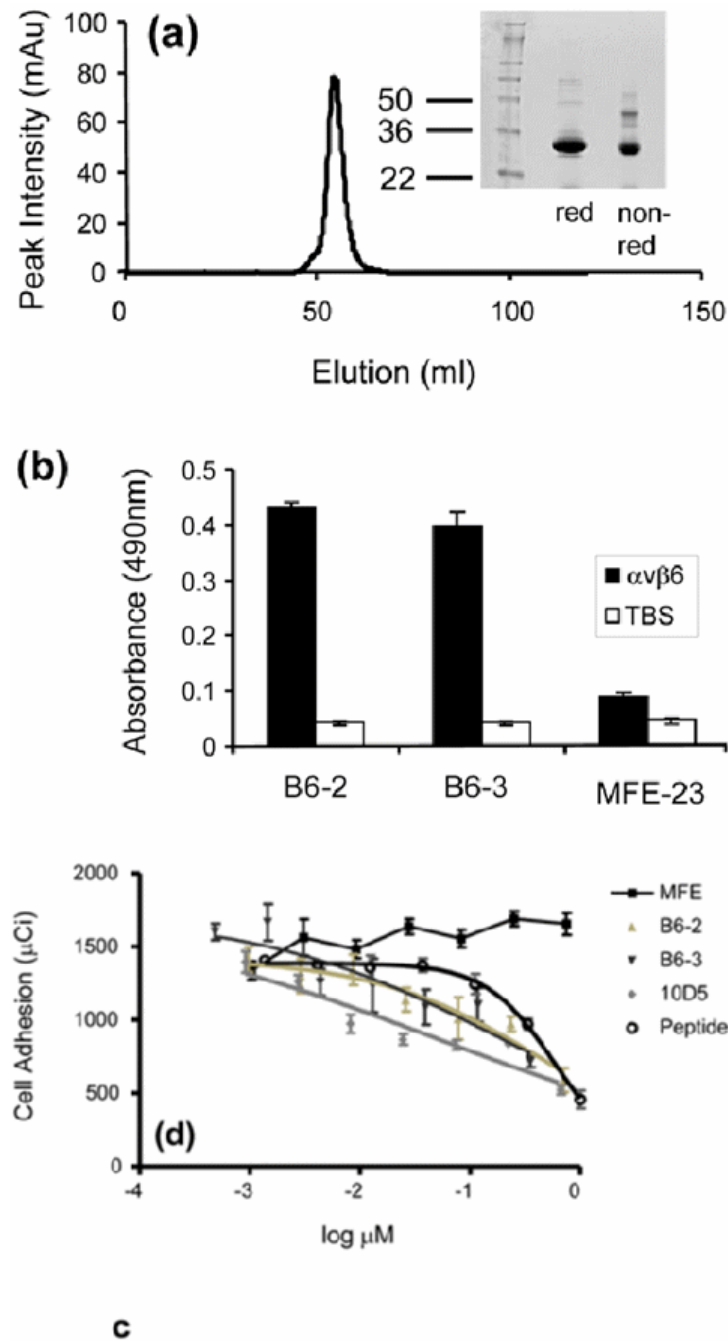


Fig. 8. Properties of B6-3. (a) Size-exclusion chromatography profile showing that B6-3 formed a dimer. Twelve percent Tri-glycine SDS-PAGE results under reducing and non-reducing conditions are shown of the dimeric fraction. (b) Chart showing that B6-3 bound to immobilized $\alpha v \beta 6$ in ELISA. B6-2, B6-3 or MFE-23 was applied at 20 $\mu\text{g/ml}$ to immobilized $\alpha v \beta 6$ and control Tris-buffered (TBS) wells. Binding was detected with mouse anti-Tetra-His IgG followed by sheep anti-mouse HRP-linked secondary antibody. The data represent the mean of triplicate measurements, and error bars represent the standard deviation at each data point. (c) Graph showing that B6-3 inhibited the adhesion of $\alpha v \beta 6$ -expressing cells to LAP. Radiolabeled [^{51}Cr] 3T3 $\beta 6.19$ cells in various concentrations of

MFE-23, B6-2, B6-3, 10D5 or the VP1 peptide A20FMDV224 were added to 96-well plates coated with 50 μ l (0.25 μ g/ml) LAP. Data show the mean and standard deviations of quadruplet wells. IC₅₀ values obtained from the experiment are as follows: A20FMDV2, 589.6 \pm 101.0 nM; B6-2, 483.5 \pm 40.5 nM; B6-3, 196.2 \pm 27.6 nM; 10D5, 51.4 \pm 32.0 nM.